AGU100 ADVANCING EARTH AND SPACE SCIENCE

Earth's Future

RESEARCH ARTICLE
10.1002/2017EF000671

Special Section:
Avoiding Disasters: Strengthening Societal Resilience to Natural Hazards

Long-Term Changes in Global Socioeconomic Benefits of Flood Defenses and Residual Risk Based on CMIP5 Climate Models

Wee Ho Lim[1,2], Dai Yamazaki[3,4], Sujan Koirala[5], Yukiko Hirabayashi[6], Shinjiro Kanae[7], Simon J. Dadson[2], Jim W. Hall[2], and Fubao Sun[1,8,9,10]

[1]Key Laboratory of Water Cycle and Related Land Surface Processes, Institute of Geographic Sciences and Natural Resources Research, Chinese Academy of Sciences, Beijing, China, [2]Environmental Change Institute, University of Oxford, Oxford, UK, [3]Institute of Industrial Science, The University of Tokyo, Tokyo, Japan, [4]Department of Integrated Climate Change Projection Research, Japan Agency for Marine-Earth Science and Technology, Yokohama, Japan, [5]Department of Biogeochemical Integration, Max Planck Institute for Biogeochemistry, Jena, Germany, [6]Department of Civil Engineering, Shibaura Institute of Technology, Tokyo, Japan, [7]Department of Civil Engineering, Tokyo Institute of Technology, Tokyo, Japan, [8]Ecology Institute of Qilian Mountain, Hexi University, Zhangye, China, [9]College of Resources and Environment, University of Chinese Academy of Sciences, Beijing, China, [10]Center for Water Resources Research, Chinese Academy of Sciences, Beijing, China

Key Points:
- The global population (GDP) exposed to flooding is ~8% (~7%) per year lower when implementing current flood protection infrastructure
- Residual population (economic) exposure is ~1% (~0.6%) of the global population (GDP) per year
- Residual risk would magnify in the globe and most of the regions (mainly where developing countries are located) in warmer worlds

Supporting Information:
- Supporting Information S1

Correspondence to:
F. Sun,
sunfb@igsnrr.ac.cn

Citation:
Lim, W. H., Yamazaki, D., Koirala, S., Hirabayashi, Y., Kanae, S., Dadson, S. J., et al. (2018). Long-term changes in global socioeconomic benefits of flood defenses and residual risk based on CMIP5 climate models. *Earth's Future*, *6*, 938–954. https://doi.org/10.1002/2017EF000671

Received 6 SEP 2017
Accepted 15 MAY 2018
Accepted article online 21 MAY 2018
Published online 2 JUL 2018

©2018. The Authors.
This is an open access article under the terms of the Creative Commons Attribution-NonCommercial-NoDerivs License, which permits use and distribution in any medium, provided the original work is properly cited, the use is non-commercial and no modifications or adaptations are made.

Abstract A warmer climate is expected to accelerate the global hydrological cycle, causing more intense precipitation and floods. Despite recent progress in global flood risk assessment, the socioeconomic benefits of flood defenses (i.e., reduction in population/economic exposure) and the residual risk (i.e., residual population/economic exposure) are poorly understood globally and regionally. To address these knowledge gaps, we use the runoff data from a baseline and 11 Coupled Model Intercomparison Project Phase 5 (CMIP5) climate models to drive the Catchment-based Macro-scale Floodplain model incorporating the latest satellite river width information. From the simulated annual maxima, we use a Gumbel distribution to estimate the river water depth-flood return period relationship. We independently evaluate flood impacts on population and economy (i.e., gross domestic product) for a range of flood return periods. We estimate the socioeconomic benefits and the corresponding residual risk for the globe and 26 subcontinental regions. The global population (gross domestic product) exposed to flooding is ~8% (~7%) per year lower when implementing existing flood protection infrastructure extracted from the FLOod PROtection Standards database. If the current flood defenses were to be unchanged in the future (Representative Concentration Pathway 4.5 [RCP4.5] and RCP8.5, i.e., ~2 to ~4.3°C above the preindustrial levels), the globe and most of the regions (particularly where developing countries are concentrated) would experience an increase in residual risk. This increase is especially obvious when the gap of climate forcing between RCP8.5 and RCP4.5 widens by the end of the 21st century. We finally evaluate the impact of changed flood defense levels on the socioeconomic benefits and the corresponding residual risk.

1. Introduction

Floods affect millions of people (Jonkman, 2005) and cost billions of dollars annually (Mills, 2005) due to extensive socioeconomic growth (Bouwer, 2011; Mohleji & Pielke, 2014) and perhaps large spatial variation in flood protection (Scussolini et al., 2016). Acceleration of the global hydrological cycle in a warmer world (e.g., Durack et al., 2012; Lim & Roderick, 2009; Oki & Kanae, 2006; Roderick et al., 2014) is projected to intensify precipitation (Allan & Soden, 2008; Allen & Ingram, 2002; Donat et al., 2016; Fischer & Knutti, 2016; O'Gorman & Schneider, 2009), causing bigger floods (Milly et al., 2002; Hirabayashi et al., 2008) with possible risk exacerbation because of socioeconomic development, land use change (e.g., deforestation and urbanization), and/or subsidence (Arnell & Gosling, 2014; Brown & Nicholls, 2015; Dixon et al., 2006; Hirabayashi et al., 2013; Ward et al., 2017; Winsemius et al., 2016). However, studies of the socioeconomic benefits of flood defenses on regional and global scales are limited. Most of the global-scale flood risk assessments focused on understanding of socioeconomic risks without flood defenses (e.g., Arnell & Gosling, 2014; Arnell & Lloyd-Hughes, 2014; Dankers et al., 2014; Hirabayashi et al., 2013; Jongman et al., 2012), while a few recent assessments have

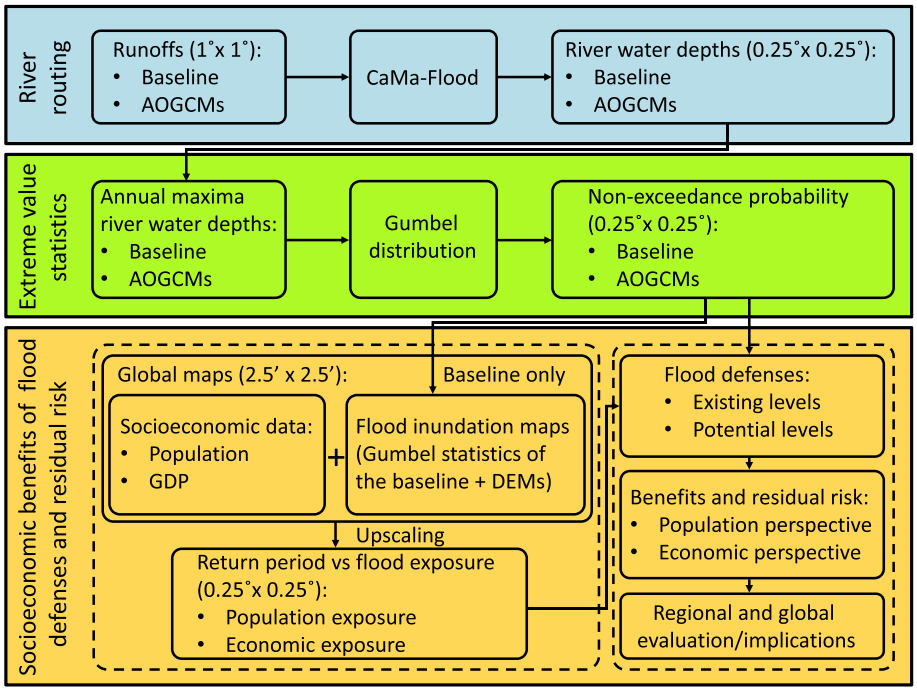

Figure 1. An overview of materials, methods, and workflow of this study (details in section 2).
AOGCM = atmosphere-ocean global circulation model; GDP = gross domestic product; DEM = digital elevation model.

begun to cover flood defenses as part of climate adaptation (e.g., European continent, Feyen et al., 2012; Rojas et al., 2013; and global, Alfieri et al., 2017; Jongman et al., 2015; Ward et al., 2017; Winsemius et al., 2016).

Nonetheless, we still do not understand how existing/potential flood defense levels would benefit the society in terms of reduction in socioeconomic exposure (e.g., population and gross domestic product [GDP]; detailed definitions in section 2.3.2). It is unclear how these numbers would evolve in different subcontinental regions (Intergovernmental Panel on Climate Change [IPCC], 2012, Table 3.A-1) and the globe under long-term climate change (e.g., by the middle and end of the 21st century). More specifically, a consistent analysis involving an ensemble of Coupled Model Intercomparison Project Phase 5 (CMIP5) climate models to quantify the effect of climate model uncertainty is not available. To our knowledge, major global reports have not explicitly addressed these policy-relevant knowledge gaps (Ghesquiere et al., 2014; IPCC, 2012, 2014a, 2014b; Sadoff et al., 2015; United Nations Office for Disaster Risk Reduction [UNISDR], 2015a). From simulation perspective, many studies (e.g., Jongman et al., 2015; Ward et al., 2017; Winsemius et al., 2016) have implemented the GLObal Flood Risk with IMAGE Scenarios (GLOFRIS) through combining the PCRaster GLOBal Water Balance model (PCR-GLOBWB; Van Beek & Bierkens, 2009) with a subgrid parameterized dynamic flow routing scheme (using kinematic wave approximation) called DynRout and a flood extent downscaling algorithm to estimate global flood hazard (detailed description in Winsemius et al., 2013). The Catchment-based Macro-scale Floodplain (CaMa-Flood) model (Yamazaki et al., 2011), which uses the diffusive wave approximation and has more advanced hydrodynamics than GLOFRIS, should complement these studies. Addressing these knowledge gaps (above) using the CaMa-Flood model should offer greater clarity on socioeconomic benefits of flood defense levels and support decision making about investments in flood risk management.

To contribute toward development of informed natural disaster risk reduction frameworks (Walch, 2015), we make an attempt to fill these knowledge gaps (above) using a simulation approach (see an overview of our approach in Figure 1; detailed description in section 2). We drive a global river routing scheme using the daily runoff output for a baseline period and atmosphere-ocean global circulation models (AOGCMs) from CMIP5 archive (Taylor et al., 2012). For a range of future climate scenarios (van Vuuren et al., 2011), we quantify the long-term change in socioeconomic benefits of flood defenses and the corresponding residual risk at ~2 to ~4.3°C above the preindustrial levels. We interpret these results for the globe and 26 subcontinental regions (Figure S1 in the supporting information).

2. Materials and Methods

2.1. Global Hydrological Modeling

Similar to Hirabayashi et al. (2013), we obtain the daily runoff data (period, 1979–2010; spatial resolution, 1° × 1°) from the Minimal Advanced Treatment of a Land Surface Interaction Runoff (Takata et al., 2003), forced by observations and reanalysis climate data (Kim et al., 2009), to represent the *baseline* runoff. We use the daily runoff data (historical period, 1960–2005; future period, 2006–2100 [2006–2099 for BCC-CSM1.1]) of 11 AOGCMs in this study (see Table 1). In the future period, we select Representative Concentration Pathway 4.5 (RCP4.5) and RCP8.5 (period 2006–2100; 2006–2099 for BCC-CSM1.1), which cover most of the key future climate scenarios in the IPCC Fourth Assessment Report (AR4) (i.e., A1T, A1B, A2, A1F1, and B2 to certain extent; IPCC, 2013, Box 1.1., their Figure 3a). For each AOGCM, we rescale the daily runoff data to 1° × 1° using bilinear interpolation. In terms of global mean surface air temperature, these periods 2046–2065 (RCP4.5), 2046–2065 (RCP8.5), 2080–2099 (RCP4.5), and 2080–2099 (RCP8.5) are ~2.0, ~2.6, ~2.4, and ~4.3°C above the preindustrial levels, respectively (IPCC, 2013, their Table SPM.2).

We apply a distributed global river routing scheme—CaMa-Flood model (Yamazaki et al., 2011; Figure S2 in the supporting information). Briefly, CaMa-Flood routes the runoff input generated by a land surface model into the oceans or lakes along a prescribed river network. It calculates the storages (river channel and floodplain), river discharge, river water depth, flood depth, and flooded area for each grid cell (spatial resolution, 0.25° × 0.25°). The river channel width data in the earlier versions of CaMa-Flood was estimated based on empirical functions of river discharges. To achieve a better consistency between river channel width data and the HydroSHEDS flow direction map in the CaMa-Flood model, a satellite river width datum called Global Width Database for Large Rivers (GWD-LR; Yamazaki et al., 2014) is incorporated into the model. We use the daily runoff data (baseline, AOGCMs) to drive the CaMa-Flood model and generate river routing outputs (see Hirabayashi et al., 2013, supporting information S1, for details of model validation). (Note that the calculation results for the CGI region [see Figure S1 in the supporting information] excludes Greenland, Iceland, and islands beyond 74°N.)

2.2. Extreme Value Statistics

Flood occurs when the flow in the river channel exceeds river channel capacity, such that excess water volume spreads across the floodplains (Figure S2 in the supporting information). In the CaMa-Flood model (also many hydrological models), the physical profile of a river and its floodplains (channel width, channel length, and floodplain elevation profile) are set constant and do not change with time. A clear relationship exists between the total water storage and the river water depth in each grid cell.

To estimate extreme value statistics in each grid cell, we use the Gumbel distribution (Gumbel, 1941), which is a member of the generalized extreme value family of distribution (Coles, 2001) and is suitable for analysis of annual maxima. Its cumulative distribution function (i.e., nonexceedance probability) is

$$F(y;\mu,\lambda) = e^{-e^{-\left(\frac{y-\mu}{\lambda}\right)}} \tag{1}$$

where y (m) is the river water depth, μ is the location parameter (dimensionless), and λ is the scale parameter (dimensionless). The parameter λ is calculated as

$$\lambda = \frac{\sqrt{6}}{\pi} s_Y = 0.7797 s_Y \tag{2}$$

and parameter μ is calculated as

$$\mu = \mu_Y - \gamma\lambda \tag{3}$$

where γ (=0.5772) is the Euler's constant (dimensionless), and μ_Y and s_Y are the mean and sample standard deviation for a collection of annual maxima $Y(=Y_1, Y_2, \ldots, Y_n)$ for the simulated river water depth output of the baseline (period, 1979–2010) and AOGCMs (period, 1970–1999) in section 2.1, respectively. Based on these parameters, we estimate the nonexceedance probability (equation (1)) of the annual maxima river water depth for the baseline and each AOGCM over the historical period and the future period (see section 2.3).

Table 1
Basic Information of AOGCMs Sourced From the CMIP5 Archive (http://cmip-pcmdi.llnl.gov/cmip5/index.html)

Model	Modeling center/group	Country	Spatial resolution†
BCC-CSM1.1	Beijing Climate Center, China Meteorological Administration	China	~2.8° × ~ 2.8° (128 × 64)
CCCma-CanESM2	Canadian Centre for Climate Modelling and Analysis	Canada	~2.8° × ~ 2.8° (128 × 64)
CMCC-CM	Centro Euro-Mediterraneo sui Cambiamenti Climatici	Italy	0.75° × 0.75° (480 × 240)
CNRM-CM5	Centre National de Recherches Meteorologiques/Centre Europeen de Recherche et Formation Advancees en Calcul Scientifique	France	~ 1.4° × ~ 1.4° (256 × 128)
CSIRO-Mk3.6.0	Commonwealth Scientific and Industrial Research Organisation in collaboration with the Queensland Climate Change Centre of Excellence	Australia	~1.9° × ~ 1.9° (192 × 96)
GFDL-ESM2G	Geophysical Fluid Dynamics Laboratory	United States	2.5° × 2° (144 × 90)
INM-CM4	Institute for Numerical Mathematics	Russia	2° × 1.5° (180 × 120)
MIROC5	Atmosphere and Ocean Research Institute, National Institute for Environmental Studies, and Japan Agency for Marine-Earth Science and Technology	Japan	~1.4° × ~ 1.4° (256 × 128)
MPI-ESM-LR	Max Planck Institute for Meteorology	Germany	~1.9° × ~ 1.9° (192 × 96)
MRI-CGCM3	Meteorological Research Institute	Japan	~1.1° × ~ 1.1° (320 × 160)
NCC-NorESM1-M	Norwegian Climate Centre	Norway	2.5° × ~1.9° (144 × 96)

Note. We include the grids in the brackets as reference. AOGCMs = atmosphere-ocean global circulation models; CMIP5 = Coupled Model Intercomparison Project Phase 5.

To estimate the specific magnitude in the nonexceedance probability of the baseline and each AOGCM, we use

$$F(y;\mu,\lambda) = 1 - \frac{1}{T} \tag{4}$$

where T (year) is the return period. We apply equation (4) to set the *threshold* for a range of flood defense levels at each grid cell (see section 2.3).

2.3. Socioeconomic Benefits of Flood Defenses and Residual Risk

2.3.1. Socioeconomic Data

To estimate the socioeconomic impacts of flooding, we use the World Bank data (country population and GDP based on purchasing power parity [PPP]) as baseline. For simplicity, we do not consider socioeconomic scenarios of future population and economic change. To prepare World Bank data with sufficiently high spatial resolution, we download the population distribution map (year, 2005; spatial resolution, 2.5′ × 2.5′ [~5 km × ~ 5 km at the equator]) from the Gridded Population of the World version 3 (GPWv3; Center for International Earth Science Information Network [CIESIN], 2005). (We weighed the availability of computing resources to cover sufficient level of details which fit the purpose of this large-scale study [section 1].) Using country mask (Freydank & Seibert, 2008), we calculate the ratio of country population from the World Bank to the sum of distributed population of each country from the GPWv3 and multiply this ratio with the population distribution of each country in GPWv3. From there, we prepare a new global population distribution map (note that data were not available for French Guiana, Taiwan, and Western Sahara). We multiply the World Bank country GDP per capita (year, 2005; unit, 2005US$ PPP) with the revised population distribution map to get a global GDP distribution map (data were not available for French Guiana, Greenland, Myanmar, North Korea, Somalia, Taiwan, and Western Sahara). Following IPCC (2012, Table 3.A-1; Figure S1 in the supporting information), we aggregate the population and GDP (constant 2005) for 26 subcontinental regions and the globe in Table 2. We note that the socioeconomic data (population and GDP) prepared here are consistent in unit (2005US$ PPP) with that of the Shared Socioeconomic Pathways (O'Neill et al., 2014), enabling future studies involving different Shared Socioeconomic Pathways to relate their estimates to the current study without handling complex unit conversion for the GDP. In addition, the year 2005 is also the final year within the historical period in the CMIP5 archive (see section 2.1), hence it is a suitable baseline to represent the recent past.

2.3.2. Benefits of Flood Defenses and Residual Risk

To estimate flood inundations, we apply the extreme value statistics of the baseline (spatial resolution, 0.25° × 0.25°; see section 2.2) and high-resolution digital elevation models (DEMs; spatial resolution, 15″ × 15″). (Briefly, these DEMs include the Shuttle Radar Topography Mission 3 arc-second DEM [SRTM3 DEM; original

Table 2
Basic Information of Land Area, Socioeconomic Data (Constant 2005), and Existing Flood Defense Levels for Each Region Defined in Figure S1

Label	Regional representation	Land area (million km^2)	Population (million)	GDP (billion 2005US$ PPP)	Flood defense levels[a] (range; median; mean; in years)
ALA	Alaska/Northwest Canada	3.36	0.6	25.5	45.7–500; 45.8; 223.8
AMZ	Amazon	8.28	65.6	651.5	0 (6.5)–33.3; 16.5; 15.2 (15.3)
CAM	Central America and Mexico	3.25	184.4	1,903.1	0 (6.5)–500; 17.6; 29.4 (29.8)
CAS	Central Asia	2.82	183.9	607.1	2–100; 10; 11.3
CEU	Central Europe	3.45	368.5	7,706.2	0 (6.5)–4,000; 49.2 (49.3); 82.1 (82.8)
CGI	East Canada, Greenland, Iceland	7.86	1.2	40.1	0 (45.7)–200; 45.7; 48.8 (48.9)
CNA	Central North America	3.98	102.7	4,527.7	17.9–500; 500; 371.5
EAF	East Africa	6.37	260.6	314.4	0 (2)–20; 2; 2.7
EAS	East Asia	8.28	1,498.8	11,455.5	0 (2)–937.8; 20; 31.2
ENA	East North America	2.66	148.7	6,400.2	0 (46.5)–500; 500; 306.2 (307.1)
MED	Southern Europe and Mediterranean	4.99	366.2	5,442.4	0 (6.5)–606.2; 16.7 (16.8); 29.2 (30.2)
NAS	North Asia	14.60	82.4	981.3	0 (6.5)–500; 45.7; 44.4
NAU	North Australia	6.31	5.2	149.9	0 (6.5)–100; 100; 99.8 (99.9)
NEB	Northeastern Brazil	2.82	75.9	802.0	16.8–38.7; 18.1; 20.1
NEU	Northern Europe	2.57	114.5	3,725.0	0 (10)–10,000; 46.4; 102.7 (103.4)
SAF	Southern Africa	6.36	139.0	611.5	0 (2)–100; 16.4; 31.4
SAH	Sahara	9.29	57.3	444.0	0 (2)–101.9; 2 (6.5); 6.4 (8.2)
SAS	South Asia	5.08	1,356.6	3,802.5	0 (2)–100; 100; 64.7
SAU	South Australia/New Zealand	2.61	20.0	623.5	100; 100; 100
SEA	Southeast Asia	5.99	510.6	3,207.0	0 (2)–163.7; 21.5 (26.5); 50.8 (52.9)
SSA	Southeastern South America	4.59	144.5	1,503.4	0 (6.5)–356.9; 17.7; 18.8
TIB	Tibetan Plateau	4.71	72.3	305.8	0 (2)–100; 20; 20.9
WAF	West Africa	7.72	338.3	871.6	0 (2)–47.1; 2.1; 5.3
WAS	West Asia	6.26	182.5	3,005.9	0 (6.5)–160.5; 17.2 (17.3); 27.5 (27.7)
WNA	West North America	5.20	79.1	3,212.9	17.6–500; 500; 304.5
WSA	West Coast South America	2.23	49.9	441.6	0 (6.5)–257.2; 17.0; 28.2 (29.1)
GLOBE	Globe (excluding Antarctica)	146.21	6,450.9	63,206.5	0 (2)–10,000; 17.1 (45.7); 51 (72.4)

[a]Source: Scussolini et al. (2016; gridded to a spatial resolution of 0.25° × 0.25°). We note that 0 here means no value, and we assume no flood defenses in such case throughout this manuscript. To understand the significance of excluding 0, we display the results in brackets if they differ from the former version as reference.
GDP = gross domestic product; PPP = purchasing power parity.

spatial resolution, 3″ × 3″] between 60°N and 60°S and the Global 30 Arc-Second Elevation Data Set [GTOPO30; original spatial resolution, 30″ × 30″] above 60°N; Hirabayashi et al., 2013). They were converted to a common spatial resolution of 15″ × 15″ using the Flexible Location of Waterways method and upscaled to 0.25° × 0.25° (Yamazaki et al., 2011). For better accuracy, we first downscale and prepare a look-up table of flood fraction (i.e., ratio of flood-inundated area to total land area per grid cell; range, 0–1; return period, 2–10,000 years) using these high-resolution DEMs. We multiply it with the population and GDP distribution maps (section 2.3.1) and upscale them to produce the look-up tables of population and economic exposure (spatial resolution, 0.25° × 0.25°). The latter step allows for relating a specific flood return period (of the baseline or AOGCMs) to population/economic exposure without repeating the similar downscaling process again.

From socioeconomic perspective, we define *benefits* as the reduction in population/economic exposure corresponding to a specific flood defense level (i.e., return period). We use the term *residual risk* to represent the residual population/economic exposure corresponding to that flood defense level. To evaluate the potential socioeconomic benefits and residual risk of flood defenses and how they might change in the long term, we use the recently assembled global flood defense database called FLOod PROtection Standards

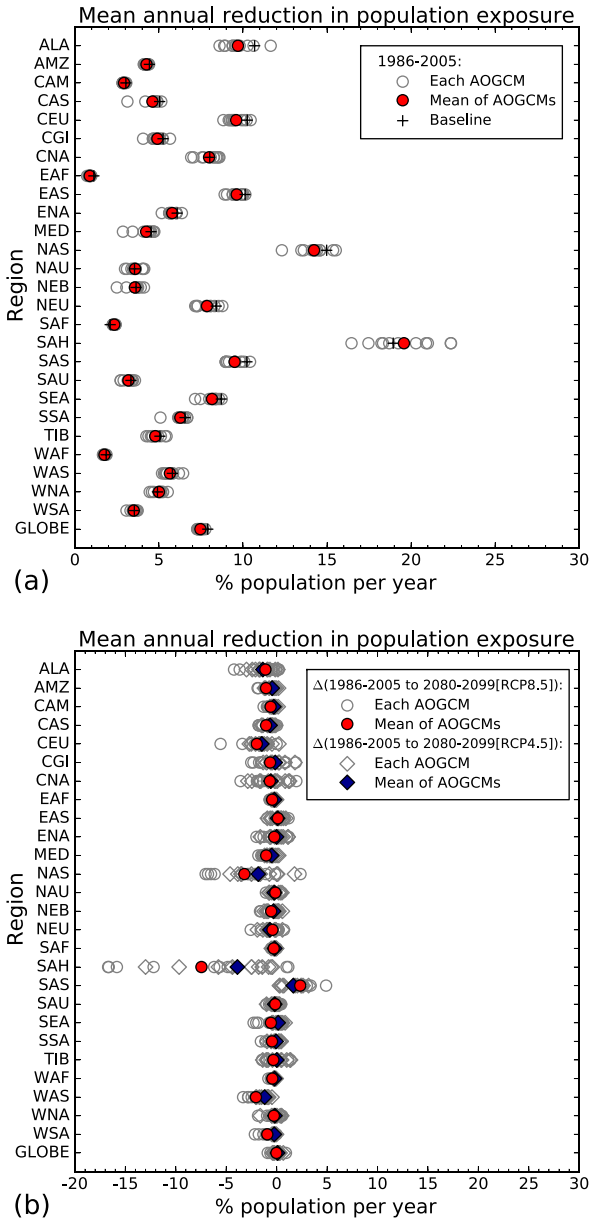

Figure 2. Reduction in population exposure at existing flood defense levels as a percentage of population per year in each region (Table 2) for (a) 1986–2005 and (b) Δ(1986–2005 to 2080–2099). AOGCM = atmosphere-ocean global circulation model; RCP = Representative Concentration Pathway.

(FLOPROS; Scussolini et al., 2016; gridded to a spatial resolution of 0.25° × 0.25°; we implemented the return period in this study) and a plausible range of flood defense levels (with return periods up to 1,000 years). When the return period of the annual maxima is less than or equal to the threshold defense level, we consider the population or economy that would have been exposed to flood inundation as the socioeconomic benefits. We quantify them by matching the return period of the annual maxima to the look-up tables of the population and economic exposure. When the return period of the annual maxima exceeds the threshold, we assume minimum socioeconomic benefits (i.e., maximum damage for the given water level) and count it toward the residual risk. We repeat the process at every grid cell of the baseline and AOGCMs. For each region and the globe (Table 2), we estimate the socioeconomic benefits and residual risk of flood defenses in the historical period (1986–2005; baseline and AOGCMs) and how they would change in the future periods (1986–2005 to 2046–2065 and 1986–2005 to 2080–2099; AOGCMs under RCP4.5 and RCP8.5). We present these estimates in terms of the mean annual value (e.g., percent population per year or percent GDP per year; see section 3).

3. Results

3.1. Benefits of Existing Flood Defenses

3.1.1. Flood Impacts on People

In the historical period (1986–2005), we find that the current flood defenses (Scussolini et al., 2016) reduce the population exposure from ~9% per year (~580 million people per year; Figure S9, subfigure *GLOBE*, label *None*, in the supporting information) to ~1% per year (~65 million people per year; Figure 3a), a reduction of ~8% per year on a global scale (Figure 2a). While the results of AOGCMs vary across regional and global scales, their ranges and ensemble means are generally consistent with that of the baseline. In the future projections (Figures 2b and S3 in the supporting information), the changes in population benefits among the AOGCMs (Δ[1986–2005 to 2046–2065] and Δ[1986–2005 to 2080–2099]) are mixed. From their ensemble means, we find that most of these regions (excluding EAS, SAS, and SEA) and the globe would experience some (often marginal) reduction in the benefits of flood protection to people under future climate conditions.

In the similar historical period, the residual population exposure ranges 0% to ~6% of the regional population per year and the global mean ~1% of the global population per year (Figure 3a), that is, on average 65 million people per year. In terms of percentage population, the regions with low flood defense levels (median ≤10 years, e.g., CAS, EAF, SAH, and WAF) would have residual population exposure above the global mean. Despite having higher flood defense levels (median ~20 years), several regions in Africa and Asia (e.g., SAF and SEA) are still susceptible to such risk. When we examine the future changes (Δ[1986–2005 to 2046–2065] and Δ[1986–2005 to 2080–2099]), we confirm that the change in regional and global residual population exposure (AOGCMs and ensemble means) generally increases with rising greenhouse gas emissions (Figures 3b and S4 in the supporting information). These outcomes indicate that flood protection infrastructure and/or emergency response capacity would need to increase in order to adapt to climate change.

3.1.2. Flood Impacts on the Economy

Based on the existing flood defenses, we repeat the above analysis, but this time we look at the economic perspective (we use percent of the regional or global GDP as proxy; Figure 4). Similarly, we find that high (low) defense level leads to high (low) economic benefits (but not always), and regional variation is visible (reaching ~22% of the regional GDP per year; Figure 4a). Globally, the current flood protection infrastructure lowered

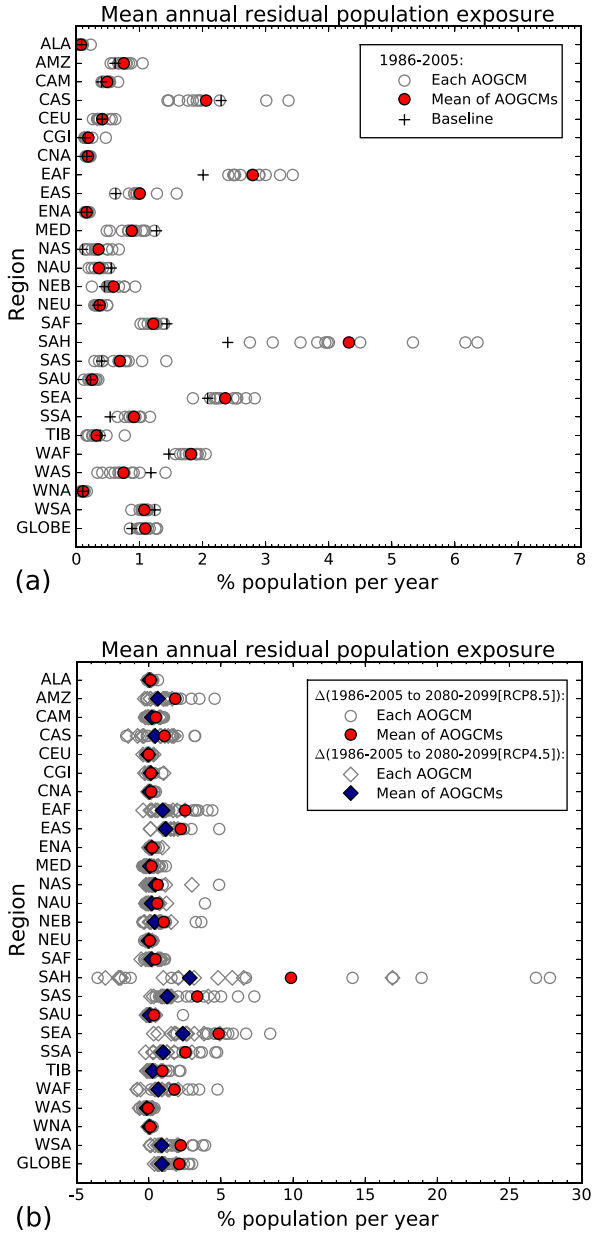

Figure 3. Residual population exposure at existing flood defense levels as a percentage of population per year in each region (Table 2) for (a) 1986–2005 and (b) Δ(1986–2005 to 2080–2099). AOGCM = atmosphere-ocean global circulation model; RCP = Representative Concentration Pathway.

the economic exposure from ~7.6% per year (~US$4.8 trillion per year; Figure S13, subfigure GLOBE, label None, in the supporting information) to ~0.6% per year (~US$0.38 trillion per year; Figure 5a), a reduction of ~7% of the global GDP per year. Again, the regional and global results of AOGCMs are in general agreement with those of the baseline. While the changes in economic benefits among the AOGCMs (Δ[1986–2005 to 2046–2065] and Δ[1986–2005 to 2080–2099]) are mixed under future climate conditions, the ensemble means show that most of the regions (except for a few regions in Asia, e.g., EAS, SAS, and SEA) and the globe would experience reduction in economic benefits (Figures 4b and S5 in the supporting information).

In the historical period (1986–2005), our estimates show that the residual economic exposure ranges 0% to ~5% of regional GDP per year, reaching about 0.6% of economy size per year (~US$0.38 trillion per year) on a global scale (Figure 5a). In terms of percentage GDP, regions with relatively low flood defense levels (median ≤10 years, e.g., CAS, EAF, SAH, and WAF) typically exceed the global mean. Several regions (e.g., SAF and SEA)

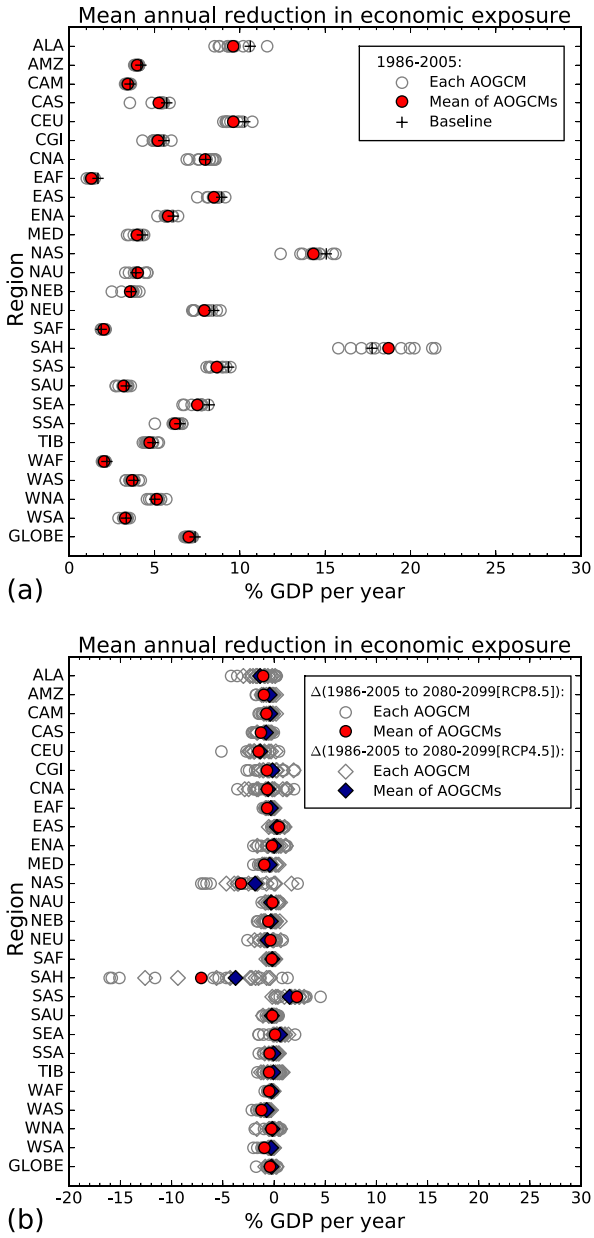

Figure 4. Reduction in economic exposure at existing flood defense levels as a percentage of GDP per year in each region (Table 2) for (a) 1986–2005 and (b) Δ(1986–2005 to 2080–2099). AOGCM = atmosphere-ocean global circulation model; RCP = Representative Concentration Pathway; GDP = gross domestic product.

are still susceptible to such risk at higher flood defense levels (median ~20 years). From the future changes (Δ[1986–2005 to 2046–2065] and Δ[1986–2005 to 2080–2099]), we find that the regional and global residual economic exposure (AOGCMs and ensemble means) would increase with rising greenhouse gas emissions (Figures 5b and S6 in the supporting information). These provide an additional dimension on rethinking the current flood risk reduction measures.

3.2. Benefits of Changing Flood Defense Levels

3.2.1. Flood Impacts on People

Next, we evaluate the impact of varied flood defense levels on population benefits. In general, the population benefits increase steeply for flood defense level ranges from the return period of 5 to 20 years, with the benefits then tailing off for the return periods of 20 to 500 years (Figure S7 in the supporting information). The ensemble mean and range of AOGCMs are close to the baseline, giving us the confidence to explore their

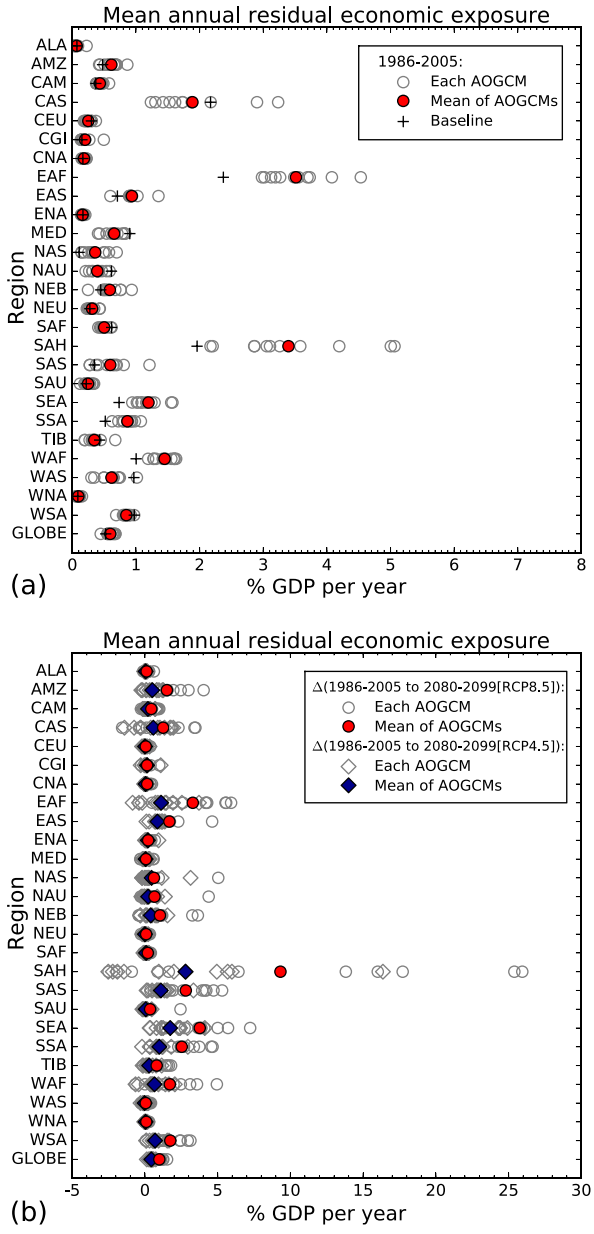

Figure 5. Residual economic exposure at existing flood defense levels as a percentage of GDP per year in each region (Table 2) for (a) 1986–2005 and (b) Δ(1986–2005 to 2080–2099). AOGCM = atmosphere-ocean global circulation model; RCP = Representative Concentration Pathway; GDP = gross domestic product.

future projections. (The reduction in population exposure of the Sahara [SAH] is substantial because of high population density in the major rivers basins. However, in common with other global flood models, flood risk is overestimated on the Nile because we do not include dam operation.) Comparing the results of future climate scenarios (RCP4.5 and RCP8.5), we confirm that higher greenhouse gas emissions would intensify the uncertainty of the change in population benefits by the middle (Figure S8 in the supporting information) and end of the 21st century (Figure 6). From the ensemble mean results (solid lines in Figures 6 and S8), we find that the population benefits would decrease at lower flood defense levels and increase at higher flood defense levels in some regions in Asia (EAS, SAS, and SEA), Africa (EAF and WAF), Latin America (AMZ, SSA, and WSA), and the globe (GLOBE) and consistently decline in several regions in North America (ALA, CAM, CGI, CNA, ENA, and WNA), Asia (CAS, NAS, and WAS), Europe/Mediterranean (NEU, CEU, and MED), and Africa (SAH). Regionally and globally, the gap between the ensemble means (of RCP4.5 and RCP8.5) might offer a general sense of the potential range of population benefits.

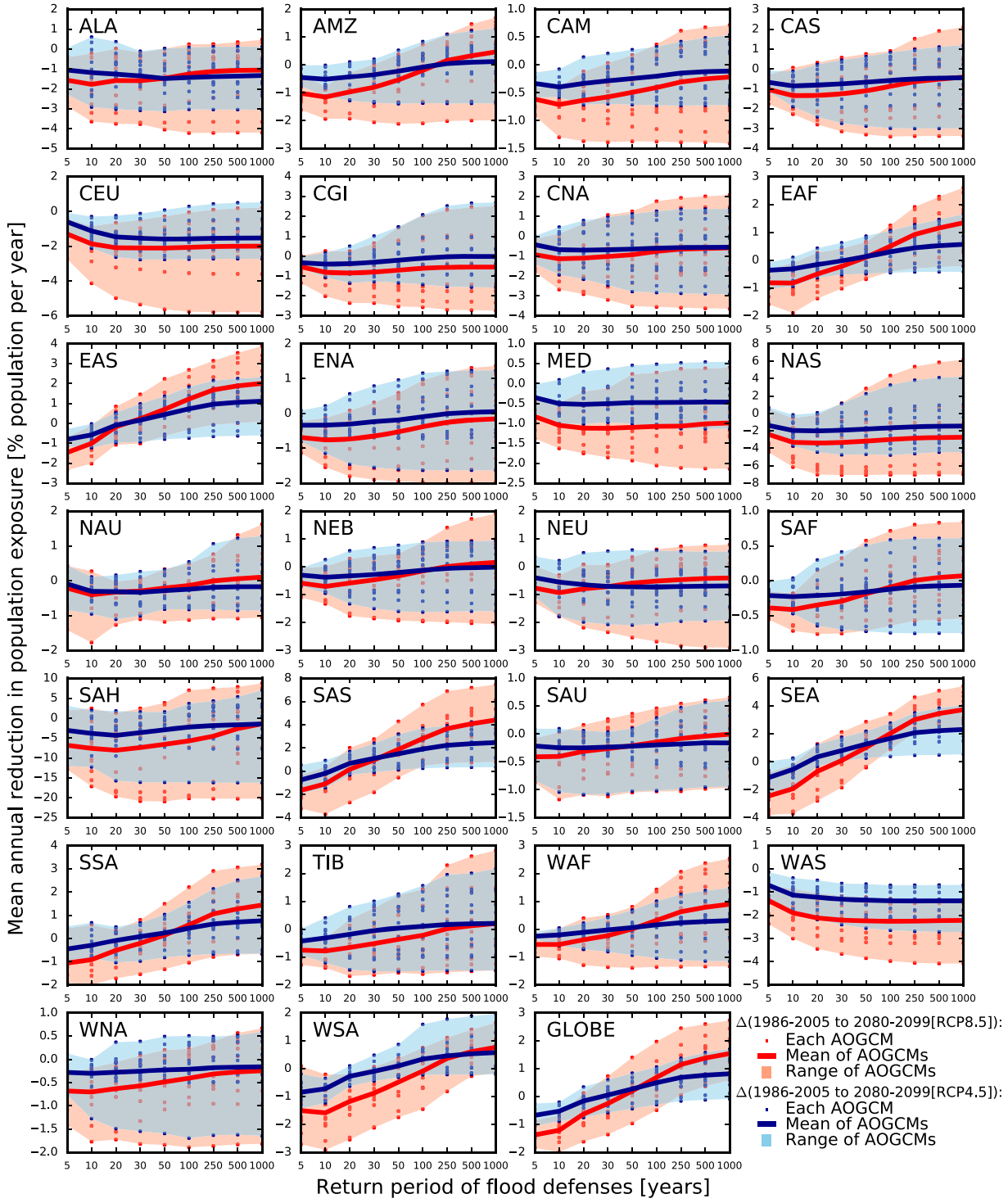

Figure 6. Reduction in population exposure versus flood defense level (expressed in return period) as a percentage of population per year in each region (Table 2) for Δ(1986–2005 to 2080–2099). AOGCM = atmosphere-ocean global circulation model; RCP = Representative Concentration Pathway.

Typically, the residual population exposure (ensemble mean and AOGCMs) declines significantly as flood defense level rises from a return period of 5 to 20 years; the decline is mild at higher flood defense levels (opposite to the population benefits in section 3.1.1; Figure S9 in the supporting information). The pattern of the ensemble mean and range of AOGCMs are consistent with that of the baseline; hence, it is reasonable to evaluate their future projections. An examination of the future scenarios (RCP4.5 and RCP8.5) shows that elevated

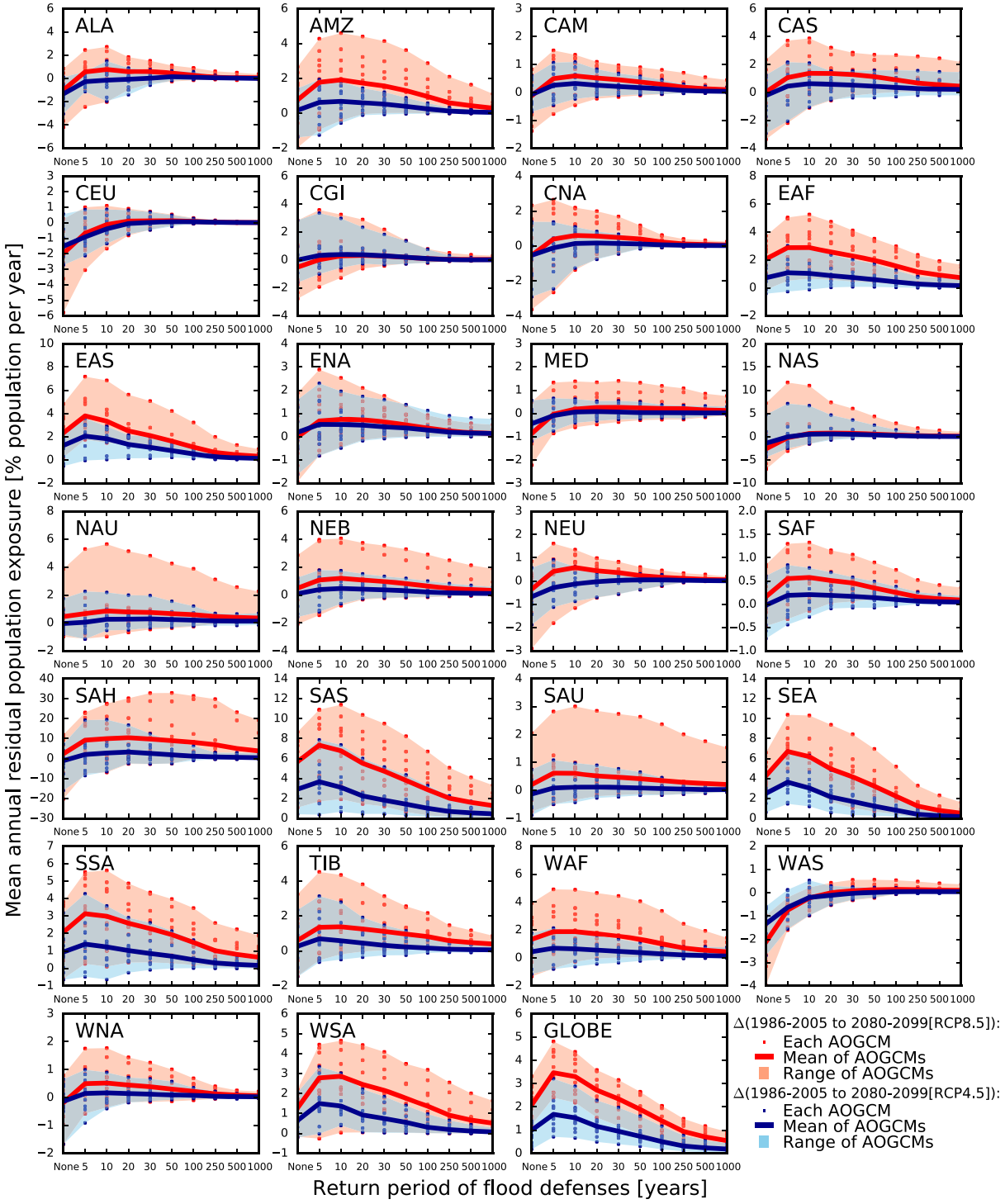

Figure 7. Residual population exposure versus flood defense level (expressed in return period) as a percentage of population per year in each region (Table 2) for Δ(1986–2005 to 2080–2099). AOGCM = atmosphere-ocean global circulation model; RCP = Representative Concentration Pathway.

greenhouse gas emissions increase the uncertainty of the change in residual population exposure by the middle (Figure S10 in the supporting information) and end of the 21st century (Figure 7). From the ensemble mean results without flood defenses (labeled None in Figures 7 and S10), the population exposure would increase in some regions (Asia [SAS and SEA], Africa [EAF and WAF], and Latin America [AMZ, SSA, and WSA]), decrease in several regions (e.g., Europe/Mediterranean [CEU, NEU, and MED], North America [ALA, CNA, and WNA],

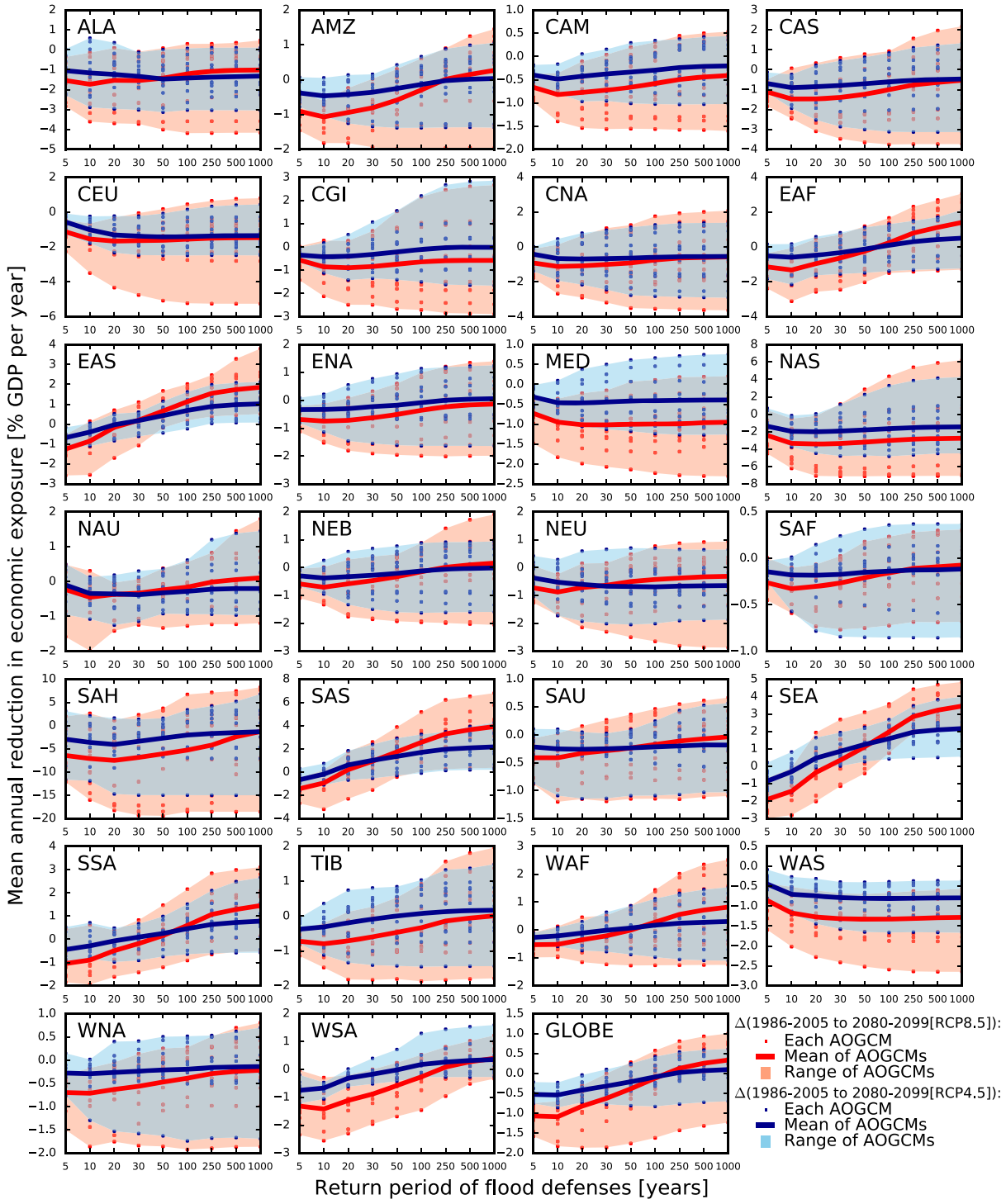

Figure 8. Reduction in economic exposure versus flood defense level (expressed in return period) as a percentage of GDP per year in each region (Table 2) for Δ(1986–2005 to 2080–2099). AOGCM = atmosphere-ocean global circulation model; RCP = Representative Concentration Pathway; GDP = gross domestic product.

and Asia [NAS and WAS]) but relatively uncertain elsewhere. The global aggregates range ~0.5% to ~1% and ~1% to ~2% of the global population by the middle and end of the 21st century, respectively. From the ensemble mean results with flood defenses, we find that the residual population exposure would increase in some parts of America (AMZ, CAM, NEB, SSA, WNA, WSA, and ENA), Asia (EAS, SAS, SEA, and TIB),

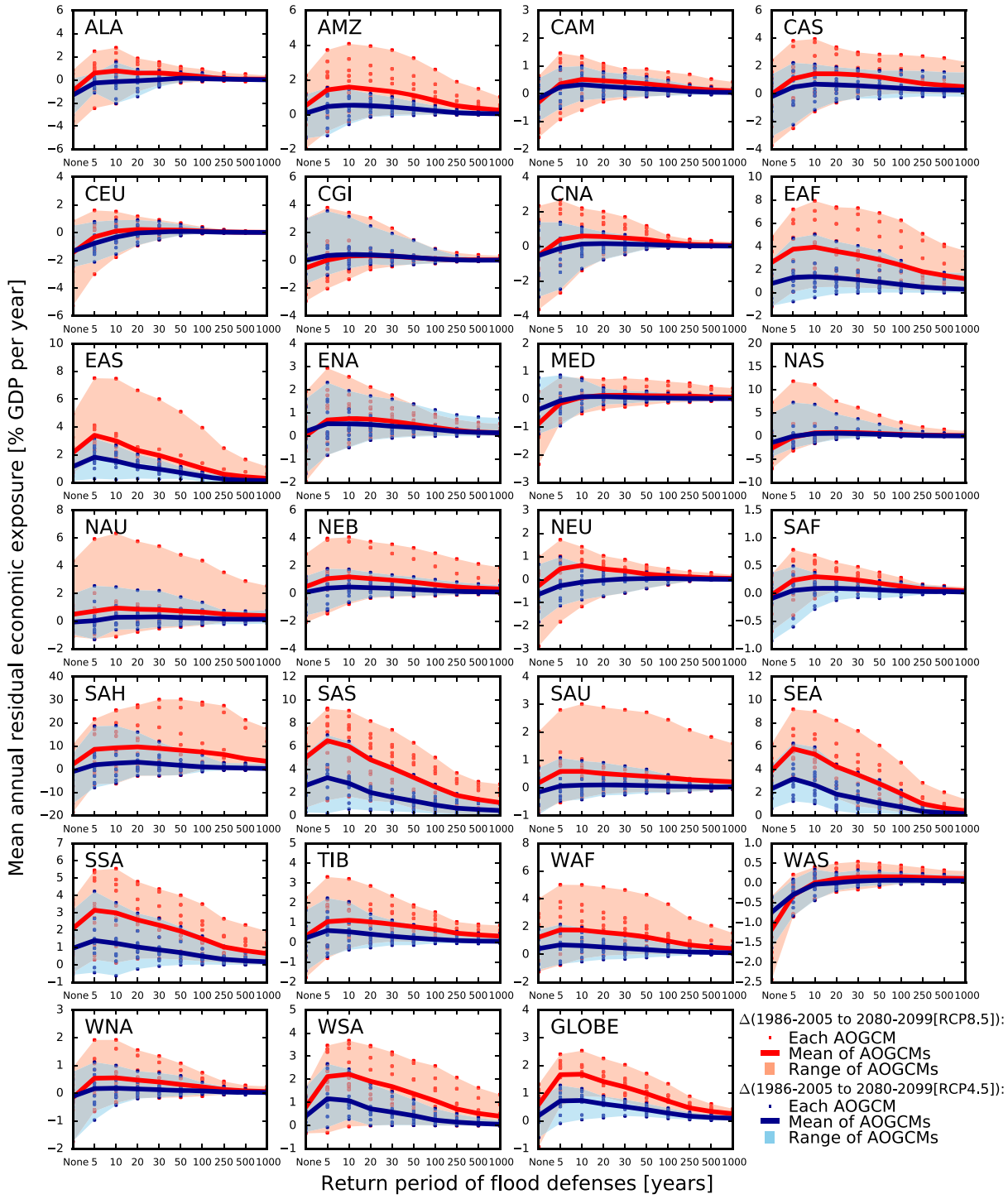

Figure 9. Residual economic exposure versus flood defense level (expressed in return period) as a percentage of GDP per year in each region (Table 2) for Δ(1986–2005 to 2080–2099). AOGCM = atmosphere-ocean global circulation model; RCP = Representative Concentration Pathway; GDP = gross domestic product.

Africa (EAF, WAF, SAF, and SAH), and the globe (GLOBE). The generalized range of residual population exposure is formed in between these ensemble means (i.e., RCP4.5 and RCP8.5).

3.2.2. Flood Impacts on the Economy

The economic benefits accelerate as the flood defense level increases from the return period of 5 to 20 years and from return period of 20 to 500 years (Figure S11 in the supporting information). (The increase in economic benefits in the Sahara [SAH] is significant because concentration of economic activities follow

the population distribution near the major river basins. Nonetheless, dam operation should have minimized the economic impacts of flooding in the Nile.) Again, the results of the future climate scenarios (RCP4.5 and RCP8.5) confirm that higher greenhouse gas emissions lead to higher uncertainty of the population benefits by the middle (Figure S12 in the supporting information) and end of the 21st century (Figure 8). From the ensemble means (solid lines in Figures 8 and S12), we find that the economic benefits fall at lower flood defense levels and rise at higher flood defense levels in some parts of Asia (EAS, SAS, and SEA), Africa (EAF and WAF), Latin America (AMZ, SSA, and WSA), and the globe (GLOBE) and consistently fall across North America (ALA, CAM, CGI, CNA, ENA, and WNA), Asia (CAS, NAS, and WAS), Europe/Mediterranean (NEU, CEU, and MED), and Africa (SAH). Regionally and globally, the gap between the ensemble means (of RCP4.5 and RCP8.5) might resemble the range of potential economic benefit.

The pattern of declining economic exposure (including ensemble mean and range of AOGCMs) with increasing flood defense levels is consistent with our general expectations (Figure S13 in the supporting information). Similar to above, the residual economic exposure declines substantially from the flood defenses with return period of 5 to 20 years and gets milder thereafter. Again, we confirm that these results are close to the baseline. The tendency of rising greenhouse gas emissions (RCP4.5 and RCP8.5) in introducing a higher uncertainty is evident with widening range of change in residual economic exposure by the middle (Figure S14 in the supporting information) and end of the 21st century (Figure 9). The ensemble mean results without flood defenses (labeled None in Figures 9 and S14) show that the economic exposure would increase in some regions (e.g., Asia [SAS and SEA], Africa [EAF and WAF], and Latin America [AMZ, NEB, SSA, and WSA]), decrease in several regions (e.g., Europe/Mediterranean [CEU, NEU, and MED], North America [ALA, CNA, and WNA), and Asia [NAS and WAS]), and be inconclusive elsewhere. The global aggregates range 0% to ~0.3% and ~0.2% to ~0.7% of the global economic size by the middle and end of the 21st century, respectively. From the ensemble mean results with flood defenses, the residual economic exposure would increase in some parts of America (AMZ, CAM, ENA, NEB, SSA, WNA, WSA, and ENA), Asia (EAS, SAS, SEA, and TIB), Africa (EAF, WAF, SAF, and SAH), and the globe (GLOBE). The gap between the ensemble means (of RCP4.5 and RCP8.5) of these results might provide insights about the potential range of residual economic exposure.

4. Discussion

4.1. Comparison With Previous Studies

With the FLOPROS database (Scussolini et al., 2016), the global aggregate of residual population exposure in the historical period (~65 million per year; see section 3.1.1) is much closer to the observed record on freshwater flooding of the Office of U.S. Foreign Disaster Assistance/Centre for Research on the Epidemiology of Disasters (OFDA/CRED) International Disaster Database (EM-DAT; Jonkman, 2005, ~81 million per year for the period 1975–2001 in Table VI [Freshwater floods]) than a recent estimate (Alfieri et al., 2017, 54 million per year), suggesting that the calculations here are more reliable. From both population and economic perspectives, our future projections concur with recent reports on concentration and elevation of (residual) risk in Africa and Asia (e.g., Alfieri et al., 2017; Hirabayashi et al., 2013), followed by some Latin American regions. These regions are home to a vast majority of the less wealthy developing countries (in terms of GDP per capita), where existing flood defense levels lag behind those of the wealthier developed countries (refer to Table 2), probably constrained by the financial capacity to invest on disaster risk reduction measures (Jongman et al., 2015). This study consistently explored the protection benefits (population and economy) and corresponding residual risk for a spectrum of flood defense levels without additional assumptions (e.g., loss function, asset valuation, and discount rate), this complements the cost-benefit analysis of Ward et al. (2017).

4.2. Limitations and Recommendations for Future Research

The outcomes of this study are broadly suitable for understanding the potential flood defense benefits and residual risk on regional and global scales. For local adaptations, details at finer spatial resolutions would be achievable through downscaling (set the boundary conditions using AOGCMs outputs) using regional climate modeling tools or statistical approaches. Considering the energy balance perspective of the climate system, advances in regional climate simulation tools (see recent review, Xie et al., 2015) might offer more insights on hydrological extremes on local scale. Depending on the local conditions, a specific flood defense infrastructure (e.g., floodgates, flood water control through dam operation, embankments, water pumping, and reservoir storage) might alter the hydrodynamics of river discharges. When such information becomes available, incorporation of this infrastructure into a hydrological model would improve the calculations. When analyzing local-scale impacts (e.g., country and small region), a combination of these hydrologic calculations

with socioeconomic data at a much higher spatial resolution (e.g., GPWv4) should offer useful quantitative insights for decision making.

We assumed that GDP distribution within each country follows the population distribution because actual spatial GDP information is scarce. Despite its simplicity, such generalization could serve as a proxy for large-scale analysis (e.g., Jongman et al., 2012; current study). Since country-based GDP per capita varies in each region, the flood impacts (e.g., benefits and residual risk) on the population and economy are also different in terms of percentage (%) and absolute value. To this end, the international organizations (e.g., United Nations and World Bank) should find both population and economic residual risk projections (see section 3) relevant for developing better targeted risk reduction goals and measures for flood-prone regions. When validated relationship between land use (e.g., rural and urban) and GDP within each country becomes available, a combination of such relationship with population distribution map might improve the assessment of flood impacts on the economy.

The FLOPROS database contains uncertainty because it consists of several layers (i.e., policy, design, and model), and local measures with high protection level (e.g., dams and reservoirs) were not included (Scussolini et al., 2016, their section 4). To a good approximation, relating the median global/regional flood defense level in the FLOPROS database (see Table 2) to the estimates in section 3.2 (e.g., Figures S7, S9, S11, and S13) would produce outcomes close to the results in section 3.1 (e.g., Figures 2a, 3a, 4a, and 5a). In a sense, the estimates in section 3.2 resemble a sensitivity analysis for the FLOPROS database. Since a logarithmic profile exists between estimated flood magnitude and return period (in section 2.2, a rearrangement of equations (1) and (4) gives $y = -\lambda \ln[-\ln(1 - \frac{1}{T})] + \mu$), these estimates are more (less) sensitive at lower (higher) flood defense levels.

The current study investigated the flood impacts of climate change and set the socioeconomic parameters constant. The data of several countries are not available and that might have affected the regional aggregation but are small for the global aggregation. Future studies could incorporate socioeconomic scenarios (O'Neill et al., 2014) and asset classes (e.g., Suwathep et al., 2015). In addition to examination of flood defense infrastructure, it would be helpful to explore the resources needed for emergency response, resilience capacity building, and/or transboundary cooperation arrangements.

5. Conclusions

Based on the most recent global river width database and CaMa-Flood model (Yamazaki et al., 2011, 2014), we independently performed a consistent analysis (overview in Figure 1) of socieconomic benefits of various flood defense levels and corresponding residual risk across the 26 subcontinental regions and the globe (Figures 2–9 and S3–S14). This comprehensive analysis addressed several knowledge gaps (see section 1) that are apparent in the IPCC Fifth Assessment Report (AR5) (IPCC, 2014a, 2014b) and the World Bank reports (Ghesquiere et al., 2014; Sadoff et al., 2015) and should complement recent studies (e.g., Alfieri et al., 2017; Arnell & Gosling, 2014; Feyen et al., 2012; Jongman et al., 2015; Rojas et al., 2013; Ward et al., 2017; Winsemius et al., 2016). In terms of CO_2 equivalent concentrations, the RCP scenarios considered here (i.e., RCP4.5 and RCP8.5) include the major Special Report on Emissions Scenarios (SRES; IPCC, 2013, see Box 1.1., Figure 3a). Hence, these findings should supplement the lack of such evaluation in the earlier IPCC special report (IPCC, 2012). Notably, the estimates Δ(1986–2005 to 2046–2065[RCP4.5]) here are directly relevant to climate change adaptations in line with the Paris Agreement's ultimate target on stabilizing global warming within 2°C above the preindustrial levels. We found stronger lift in residual risk for the globe and most of the regions under higher greenhouse gas emissions scenario (RCP8.5), particularly in subcontinental regions where most developing countries are located. The insights into regional variation should support decision making on climate change adaptations (priorities in UNISDR, 2015b; e.g., water infrastructure investment, flood warning system, and emergency and resilience capacity building). Moreover, expectation of reduced global residual risk under lower greenhouse gas emission scenario (such as RCP4.5 or lower) should motivate climate change mitigation efforts at international level (United Nations, 2015).

Acknowledgments
This study was financially supported by the National Key Research and Development Program of China (2016YFA0602402), the Oxford Martin Programme on Resource Stewardship in the Oxford Martin School, the Chinese Academy of Sciences President's International Fellowship Initiative (W. H. L., 2017PC0068), the Chinese Academy of Sciences Pioneer Hundred Talents Program (F. S.), and the Environmental Research and Technology Development Fund (Y. H., S-14, MiLAi) of the Ministry of the Environment, Japan. We thank Sen Li, Michael Gilmont, Raghav Pant, Michael Simpson, and Matthew Ives for helpful discussions. We are very grateful to an anonymous reviewer for helpful comments. We acknowledge the World Climate Research Programme's Working Group on Coupled Modelling, which is responsible for CMIP, and we thank the climate modeling groups (Table 1 in this manuscript) for producing and making available their model output. For CMIP the U.S. Department of Energy's Program for Climate Model Diagnosis and Intercomparison provides coordinating support and led development of software infrastructure in partnership with the Global Organization for Earth System Science Portals. The CMIP5 climate models used in this study are sourced from http://cmip-pcmdi.llnl.gov/cmip5/index.html. The CaMa-Flood model and GWD-LR data set are accessible at http://hydro.iis.u-tokyo.ac.jp/~yamadai/cama-flood/. The FLOPROS data set can be downloaded from the Supplement section of Scussolini et al. (2016): https://www.nat-hazards-earth-syst-sci.net/16/1049/2016/. The GPWv3 population data are available here: http://sedac.ciesin.columbia.edu/data/collection/gpw-v3. The World Bank country population and GDP data can be downloaded from https://data.worldbank.org/.

References

Alfieri, L., Bisselink, B., Dottori, F., de Roo Naumann, A., Salamon, P., Wyser, K., & Feyen, L. (2017). Global projections of river flood risk in a warmer world. *Earth's Future*, *5*, 171–182. https://doi.org/10.1002/2016EF000485

Allan, R. P., & Soden, J. (2008). Atmospheric warming and the amplification of precipitation extremes. *Science*, *321*, 1481–1484. https://doi.org/10.1126/science.1160787

Allen, M. R., & Ingram, W. J. (2002). Constraints on future changes in climate and the hydrological cycle. *Nature*, *419*, 224–590. https://doi.org/10.1038/nature01092

Arnell, N. W., & Gosling, S. N. (2014). The impacts of climate change on river flood risk at the global scale. *Climatic Change*, *123*, 387–401. https://doi.org/10.1007/s10584-014-1084-5

Arnell, N. W., & Lloyd-Hughes, B. (2014). The global-scale impacts of climate change on water resources and flooding under new climate and socio-economic scenarios. *Climatic Change*, *122*, 127–140. https://doi.org/10.1007/s10584-013-0948-4

Bouwer, L. M. (2011). Have disaster losses increased due to anthropogenic climate change? *Bulletin of American Meteorological Society*, *92*, 39–46. https://doi.org/10.1175/2010BAMS3092.1

Brown, S., & Nicholls, R. J. (2015). Subsidence and human influences in mega deltas: The case of the Ganges-Brahmaputra-Meghna. *Science of the Total Environment*, *527-528*, 362–374. https://doi.org/10.1016/j.scitotenv. 2015.04.124

CIESIN (2005). *CIESIN-Columbia University, FAO, CIAT. Gridded population of the world, version 3 (GPWv3): Population Count Grid*. Palisades, New York: NASA Socioeconomic Data and Applications Center (SEDAC). https://doi.org/10.7927/H4639MPP

Coles, S. (2001). *An introduction to statistical modeling of extreme values*. London: Springer. https://doi.org/10.1007/978-1-4471-3675-0

Dankers, R., Arnell, N. W., Clark, D. B., Falloon, P. D., Fekete, B. M., Gosling, S. N., & Wisser, D. (2014). First look at changes in flood hazard in the Inter-Sectoral Impact Model Intercomparison Project ensemble. *Proceedings of the National Academy of Sciences of the United States of America*, *111*, 3257–3261. https://doi.org/10.1073/pnas.1302078110

Dixon, T. H., Amelung, F., Ferretti, A., Novali, F., Rocca, F., Dokka, R., & Whitman, D. (2006). Space geodesy: Subsidence and flooding in New Orleans. *Nature*, *441*, 587–588. https://doi.org.10.1038/441587a

Donat, M. G., Lowry, A. L., Alexander, L. V., O'Gorman, P. A., & Maher, N. (2016). More extreme precipitation in the world's dry and wet regions. *Nature Climate Change*, *6*, 508–513. https://doi.org/10.1038/NCLIMATE2941

Durack, P. J., Wijffels, S. E., & Matear, R. J. (2012). Ocean salinities reveal strong global water cycle intensification during 1950 to 2000. *Science*, *334*, 455–458. https://doi.org/10.1126/science.1212222

Feyen, L., Dankers, R., Bódis, K., Salamon, P., & Barredo, J. I. (2012). Fluvial flood risk in Europe in present and future climates. *Climatic Change*, *112*, 47–62. https://doi.org/10.1007/s10584-011-0339-7

Fischer, E. M., & Knutti, R. (2016). Observed heavy precipitation increase confirms theory and early models. *Nature Climate Change*, *6*, 986–991. https://doi.org/10.1038/NCLIMATE3110

Freydank, K., & Seibert, S. (2008). *Towards mapping the extent of irrigation in the last century: A time series of irrigated area per country*. Frankfurt, Germany: Institute of Physical Geography University of Frankfurt.

Ghesquiere, F., Simpson, A. L., Phillips, E. K., Toro Landivar, J. C. J., Wyan, A. A., Balog, S. A. B., & Heslop, C. (2014). Understanding risk: Producing actionable information—Proceedings from the 2014 UR forum, World Bank Group, Washington, DC. Retrieved from http://documents.worldbank.org/curated/en/486381468183897622/Understanding-risk-producing-actionable-information-proceedings-from-the-2014-UR-forum, last access in May 2018.

Gumbel, E. J. (1941). The return period of flood flows. *The Annals of Mathematical Statistics*, *12*, 163–190.

Hirabayashi, Y., Kanae, S., Emori, S., Oki, T., & Kimoto, M. (2008). Global projections of changing risks of floods and droughts in a changing climate. *Hydrological Sciences Journal*, *53*, 754–772. https://doi.org/10.1623/hysj.53.4.754

Hirabayashi, Y., Mahendran, R., Koirala, S., Konoshima, L., Yamazaki, D., Watanabe, S., & Kanae, S. (2013). Global flood risk under climate change. *Nature Climate Change*, *3*, 816–821. https://doi.org/10.1038/NCLIMATE1911

IPCC (2012). Managing the risks of extreme events and disasters to advance climate change adaptation. In C. B. Field, et al. (Eds.), *A special report of Working Groups I and II of the Intergovernmental Panel on Climate Change*. Cambridge, UK and New York: Cambridge University Press.

IPCC (2013). Climate change 2013: The physical science basis. In T. F. Stocker, et al. (Eds.), *Contribution of Working Group I to the Fifth Assessment Report of the Intergovernmental Panel on Climate Change*. Cambridge, UK and New York: Cambridge University Press. https://doi.org/10.1017/CBO9781107415324

IPCC (2014a). Climate change 2014: Impacts, adaptation, and vulnerability. Part A: Global and sectoral aspects. In C. B. Field, et al. (Eds.), *Contribution of Working Group II to the Fifth Assessment Report of the Intergovernmental Panel on Climate Change*. Cambridge, UK and New York: Cambridge University Press.

IPCC (2014b). Climate change 2014: Impacts, Adaptation, and Vulnerability. Part B: Regional Aspects. In V. R. Barros, et al. (Eds.), *Contribution of Working Group II to the Fifth Assessment Report of the Intergovernmental Panel on Climate Change*. Cambridge, UK and New York: Cambridge University Press.

Jongman, B., Ward, P. J., & Aerts, J. C. J. H. (2012). Global exposure to river and coastal flooding: Long term trends and changes. *Global Environmental Change*, *22*, 823–835. https://doi.org/10.1016/j.gloenvcha.2012.07.004

Jongman, B., Winsemius, H. C., Aerts, J. C. J. H., de Perez, E. C., van Aalst, M. K., Kron, W., & Ward, P. J. (2015). Declining vulnerability to river floods and the global benefits of adaptation. *Proceedings of the National Academy of Sciences of the United States of America*, *112*, E2271–E2280. https://doi.org/10.1073/pnas.1414439112

Jonkman, S. N. (2005). Global perspective on loss of human life caused by floods. *Natural Hazards*, *34*, 151–175. https://doi.org/10.1007/s11069-004-8891-3

Kim, H., Yeh, P.-F., Oki, T., & Kanae, S. (2009). Role of rivers in the seasonal variations of terrestrial water storage over global basins. *Geophysical Research Letters*, *36*, L17402. https://doi.org/10.1029/2009GL039006

Lim, W. H., & Roderick, M. L. (2009). An atlas of the global water cycle: Based on the IPCC AR4 models, ANU E-Press, Canberra. Retrieved from http://epress.anu.edu.au/global_water_cycle_citation.html, last access in May 2018.

Mills, E. (2005). Insurance in a climate of change. *Science*, *309*, 1040–1044. https://doi.org/10.1126/science.1112121

Milly, P. C. D., Wetherald, R. T., Dunne, K. A., & Delworth, T. L. (2002). Increasing risk of great floods in a changing climate. *Nature*, *415*, 514–517. https://doi.org/10.1038/415514a

Mohleji, S., & Pielke, R. A. (2014). Reconciliation of trends in global and regional economic losses from weather events: 1980–2008. *Natural Hazards Review*, *15*, 04014009. https://doi.org/10.1061/(ASCE)NH.1527-6996.0000141

O'Gorman, P. A., & Schneider, T. (2009). The physical basis for increases in precipitation extremes in simulations of 21st-century climate change. *Proceedings of the National Academy of Sciences of the United States of America*, *106*, 14,773–14,777. https://doi.org/10.1073/pnas.0907610106

O'Neill, B. C., Kriegler, E., Riahi, K., Ebi, K. L., Hallegatte, S., Carter, T. R., & van Vuuren, D. P. (2014). A new scenario framework for climate change research: The concept of shared socioeconomic pathways. *Climatic Change*, *122*, 387–400. https://doi.org/10.1007/s10584-013-0905-2

Oki, T., & Kanae, S. (2006). Global hydrological cycles and world water resources. *Science*, *313*, 1068–1072. https://doi.org/10.1126/science.1128845

Roderick, M. L., Sun, F., Lim, W. H., & Farquhar, G. D. (2014). A general framework for understanding the response of the water cycle to global warming over land and ocean. *Hydrology and Earth System Sciences*, *18*, 1575–1589. https://doi.org/10.5194/hess-18-1575-2014

Rojas, R., Feyen, L., & Watkiss, P. (2013). Climate change and river floods in the European Union: Socio-economic consequences and the costs and benefits of adaptation. *Global Environmental Change*, *23*, 1737–1751. https://doi.org/10.1016/j.gloenvcha.2013.08.006

Sadoff, C. W., Hall, J. W., Grey, D., Aerts, J. C. J. H., Ait-Kadi, M., Brown, C., et al. (2015). *Securing water, sustaining growth: Report of the GWP/OECD Task Force on Water Security and Sustainable Growth*. UK: University of Oxford.

Scussolini, P., Aerts, J. C. J. H., Jongman, B., Bouwer, L. M., Winsemius, H. C., de Moel, H., & Ward, P. J. (2016). FLOPROS: An evolving global database of flood protection standards. *Natural Hazards and Earth System Sciences*, *16*, 1049–1061. https://doi.org/10.5194/nhess-16-1049-2016

Suwathep, T., Lim, W. H., Iseri, Y., & Kanae, S. (2015). Generalized method to estimate value of urban assets for natural disaster risk assessment at the macro scale. *Hydrological Research Letters*, *9*, 103–106. https://doi.org/10.3178/hrl.9.103

Takata, K., Emori, S., & Watanabe, T. (2003). Development of the minimal advanced treatments of surface interaction and runoff. *Global Planetary Change*, *38*, 209–222. https://doi.org/10.1016/S0921-8181(03) 00030-4

Taylor, K. E., Stouffer, R. J., & Meehl, G. A. (2012). An overview of CMIP5 and the experiment design. *Bulletin of the American Meteorological Society*, *93*, 485–498. https://doi.org/10.1175/BAMS-D-11-00094.1

United Nations (2015). Synthesis report on the aggregate effect of the intended nationally determined contributions, FCCC/CP/2015/7. Retrieved from http://unfccc.int/resource/docs/2015/cop21/eng/07.pdf, last access in May 2018.

UNISDR (2015a). *Making development sustainable: The future of disaster risk management. Global assessment report on disaster risk reduction*. Geneva, Switzerland: United Nations Office for Disaster Risk Reduction (UNISDR).

UNISDR (2015b). Sendai framework for disaster risk reduction 2015–2030. Retrieved from http://www.preventionweb.net/files/43291_sendaiframeworkfordrren.pdf, last access in May 2018.

Van Beek, L. P. H., & Bierkens, M. F. P. (2009). Department of Physical Geography, Utrecht University, Netherlands, The global hydrological model PCR-GLOBWB: Conceptualization, parameterization and verification. Retrieved from http://vanbeek.geo.uu.nl/suppinfo/vanbeekbierkens2009.pdf, last access in May 2018.

van Vuuren, D. P., Edmonds, J., Kainuma, M., Riahi, K., Thomson, A., Hibbard, K., & Rose, S. K. (2011). The representative concentration pathways: An overview. *Climatic Change*, *109*, 5–31. https://doi.org/10.1007/s10584-011-0148-z

Walch, C. (2015). Expertise and policy-making in disaster risk reduction. *Nature Climate Change*, *5*, 706–707. https://doi.org/10.1038/NCLIMATE2680

Ward, P. J., Jongman, B., Aerts, J. C. J. H., Bates, P. D., Botzen, W. J. W., Loaiza, A. D., & Winsemius, H. C. (2017). A global framework for future costs and benefits of river-flood protection in urban areas. *Nature Climate Change*, *7*, 642–646. https://doi.org/10.1038/NCLIMATE3350

Winsemius, H. C., van Beek, L. P. H., Bierkens, M. F. P., Bouwman, A., Jongman, B., & Ward, P. J. (2016). Global drivers of future flood risk. *Nature Climate Change*, *6*, 381–385. https://doi.org/10.1038/NCLIMATE2893

Winsemius, H. C., Van Beek, L. P. H., Jongman, B., Ward, P. J., & Bouwman, A. (2013). A framework for global river flood risk assessments. *Hydrology and Earth System Sciences*, *17*, 1871–1892. https://doi.org/10.5194/hess-17-1871-2013

Xie, S.-P., Deser, C., Vecchi, G. A., Collins, M., Delworth, T. L., Hall, A., & Watanabe, M. (2015). Towards predictive understanding of regional climate change. *Nature Climate Change*, *5*, 921–930. https://doi.org/10.1038/NCLIMATE2689

Yamazaki, D., Kanae, S., Kim, H., & Oki, T. (2011). A physically based description of floodplain inundation dynamics in a global river routing model. *Water Resources Research*, *47*, W04501. https://doi.org/10.1029/2010WR009726

Yamazaki, D., O'Loughlin, F., Trigg, M. A., Miller, Z. F., Pavelsky, T. M., & Bates, P. D. (2014). Development of the Global Width Database for Large Rivers. *Water Resources Research*, *50*, 3467–3480. https://doi.org/10.1002/2013WR014664